Supplementary Materials for

The Adsorption of Durene and Prehnitene on Metal-organic Frameworks

The optimized structures of MOFs

The structures of MOFs were optimized by VASP software. Then the skeletons were expanded to 2×2×1 supercell and kept rigid during simulation to satisfy periodic boundary conditions. The optimized structures were shown in Figure S1.

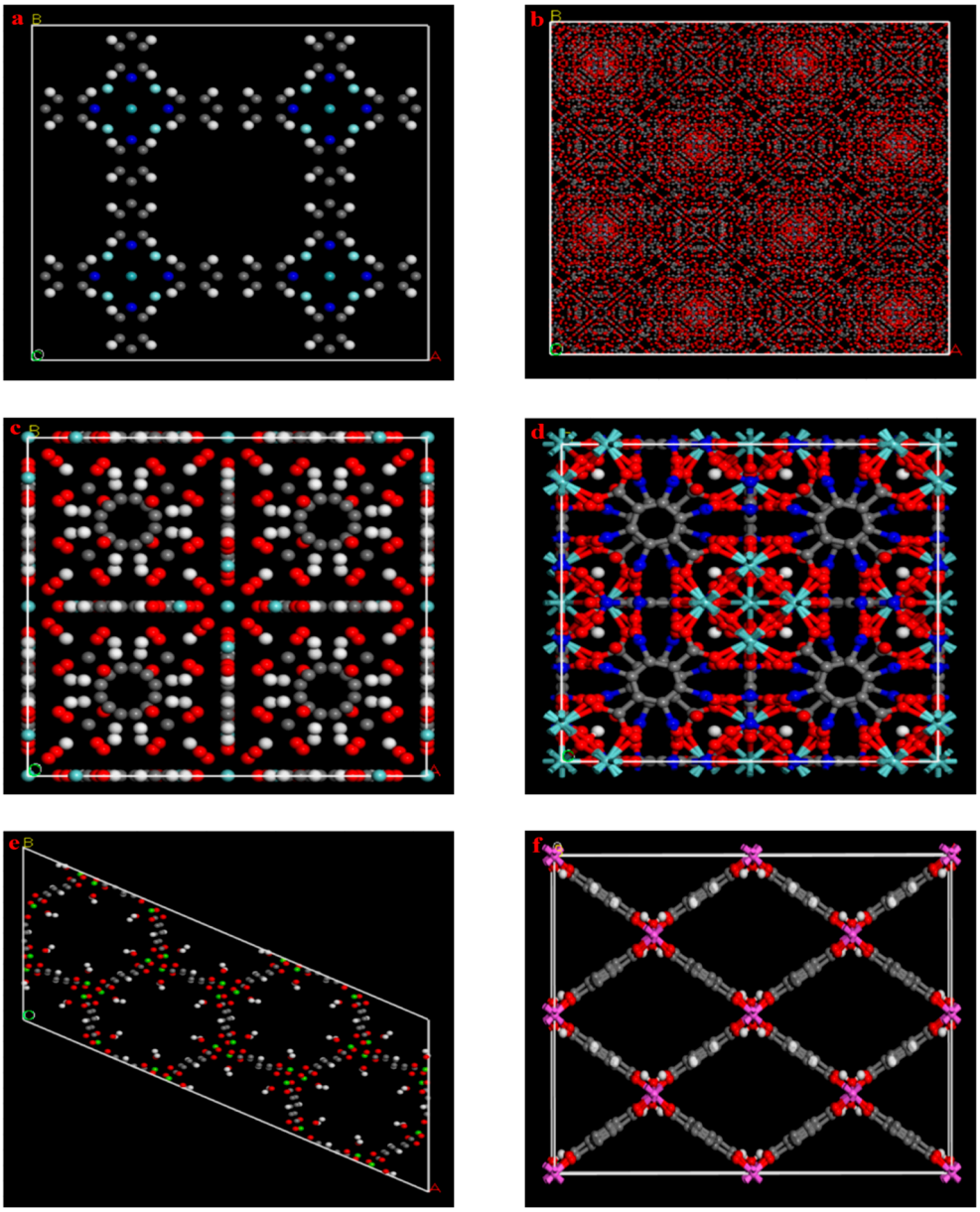

Figure S1. Optimized Structures of MOFs:
(a) ZU-61; (b) MIL-101; (c) UIO-66; (d) UIO-66-NH_2; (e) Mg-MOF-74; (f) Al-MIL-53

The atomic charges of DR and PR

The optimized structures of DR and PR were shown in Fig. S2. The atomic charges were calculated by QEq method and listed in Table S1.

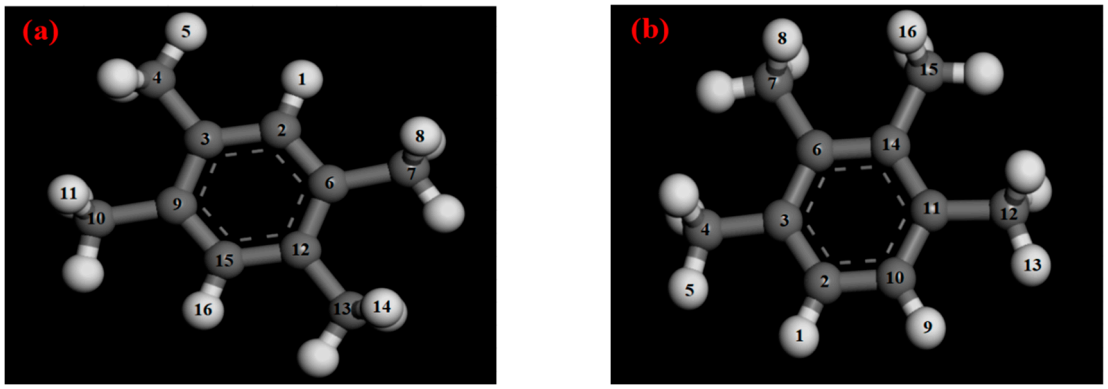

Figure S2. Optimized structures of tetratoluene: (a) DR; (b) PR

Table S1. Atomic charges of DR and PR

	charge(e)	
	DR	PR
1	0.0938	0.0959
2	-0.0962	-0.1104
3	0.0334	0.0341
4	-0.4018	-0.4023
5	0.1223	0.1212
6	0.0334	0.0462
7	-0.4018	-0.3972
8	0.1223	0.1170
9	0.0334	0.0959
10	-0.4018	-0.1104
11	0.1223	0.0341
12	0.0334	-0.4023
13	-0.4018	0.1212
14	0.1223	0.0462
15	-0.0962	-0.3972
16	0.0938	0.1170

The adsorption capacity of mixture

The adsorption capacity of mixture on six MOFs from 10 kPa to 300 kPa were calculated and listed in Table S2.

Table S2 Adsorption capacity of DR and PR from 10 kPa to 300 kPa

Pressure (kPa)	Adsorption capacity(mg/g)											
	ZU-61		MIL-101		UIO-66-NH_2		Al-MIL-53		Mg-MOF-74		UIO-66	
	DR	PR	DR	PR	DR	PR	DR	PR	DR	PR	DR	PR
10	33.29	60.24	62.90	65.49	34.78	22.33	144.46	200.05	43.52	55.08	57.78	31.03
39	50.89	99.26	78.37	81.64	45.33	30.68	162.37	223.49	57.24	73.24	73.06	38.78
68	64.33	128.24	90.74	95.32	53.09	35.24	177.53	247.51	65.90	87.33	89.37	47.57
97	70.78	153.33	107.33	110.94	58.98	38.65	195.30	264.99	72.37	99.02	101.82	54.03
126	76.33	176.36	123.84	128.24	61.84	40.03	210.43	285.45	80.22	120.36	117.39	60.99
155	83.13	194.67	146.26	152.38	65.36	42.80	217.75	299.59	85.54	132.38	130.79	66.38
184	93.78	222.40	164.35	170.26	68.72	44.58	223.55	306.83	89.95	147.98	141.83	71.14
213	97.71	233.15	179.29	186.48	74.56	45.06	228.75	314.49	92.33	156.73	146.32	75.39
242	103.76	245.07	189.15	193.64	77.34	46.29	234.68	320.37	95.33	162.89	150.39	79.33
271	109.24	257.42	194.07	199.72	79.24	47.24	239.89	323.00	99.35	170.38	156.83	82.15
300	110.85	261.39	196.20	204.05	80.03	48.38	241.48	324.58	100.14	176.67	158.81	83.44

The pore size distribution of synthesized MOFs

The selected MOFs(UIO-66, UIO-66-NH_2, Mg-MOF-74, and ZU-61) were synthesized by solvethermal method, which were shown in Figure S3. Then the pore size distribution of synthesized materials were calculated by Horvath-Kawazoe methods and plotted in Figure S4.



Figure S3. The snapshot of four synthesized MOFs:
(a) UIO-66; (b) UIO-66-NH_2; (c) Mg-MOF-74; (d) ZU-61

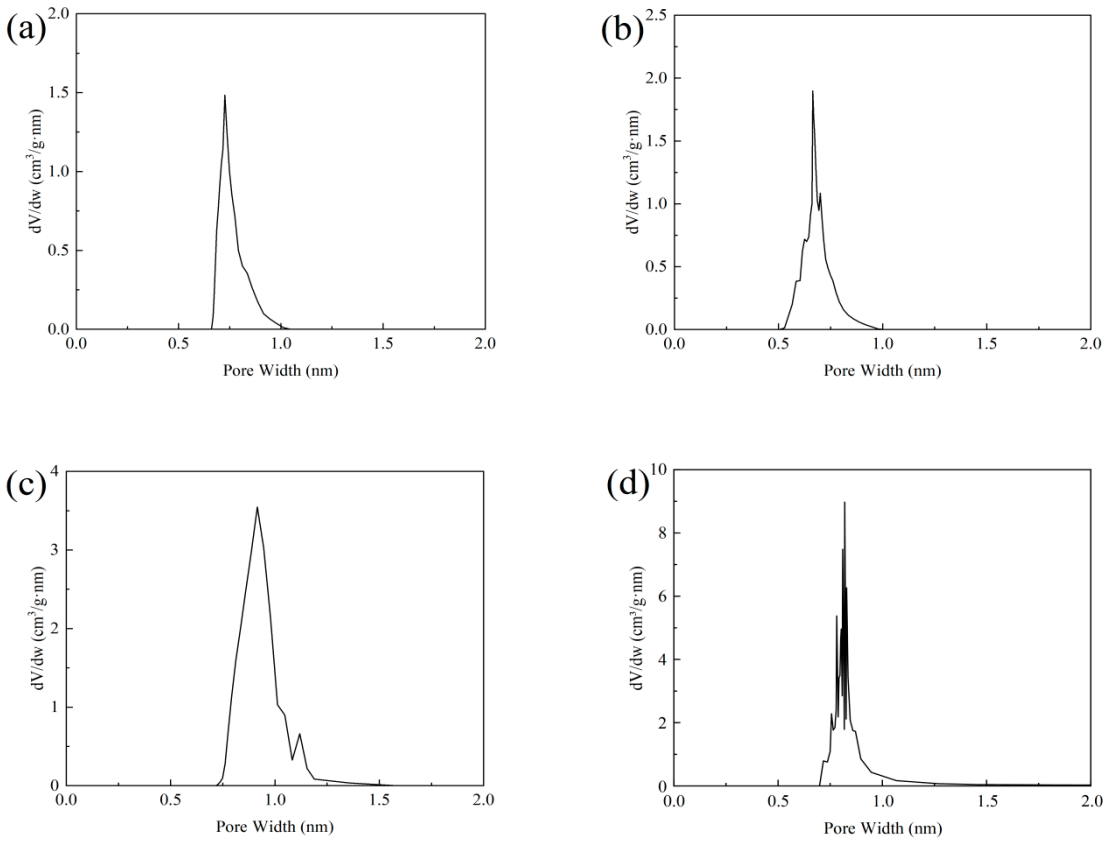

Figure S4. The pore size distribution of four MOFs:
(a) UIO-66; (b) UIO-66-NH_2; (c) Mg-MOF-74; (d) ZU-61